

Response of the Brazilian gravitational wave detector to signals from a black hole ringdown

César A Costa¹, Odylio D Aguiar¹ and Nadja S Magalhães²

¹ Divisão de Astrofísica, Instituto Nacional de Pesquisas Espaciais, Av. dos Astronautas, 1758, Jd Granja, CEP 12227-010, São José dos Campos, SP, Brazil

² Departamento de Física, Instituto Tecnológico de Aeronáutica, Praça Marechal Eduardo Gomes, 50, Vila das Acácias, CEP 12228-900, São José dos Campos, SP, Brazil

E-mail: cesar@das.inpe.br, odylio@das.inpe.br and nadjam@ita.br

Received 31 August 2003

Published 10 February 2004

Online at stacks.iop.org/CQG/21/S827 (DOI: 10.1088/0264-9381/21/5/066)

Abstract

It is assumed that a black hole can be disturbed in such a way that a ringdown gravitational wave would be generated. This ringdown waveform is well understood and is modelled as an exponentially damped sinusoid. In this work, we use this kind of waveform to study the performance of the SCHENBERG gravitational wave detector. This first realistic simulation will help us to develop strategies for the signal analysis of this Brazilian detector. We calculated the signal-to-noise ratio as a function of frequency for the simulated signals and obtained results that show that SCHENBERG is expected to be sensitive enough to detect this kind of signal up to a distance of ~ 20 kpc.

PACS numbers: 04.80.Nn, 95.55.Ym

(Some figures in this article are in colour only in the electronic version)

1. Black hole ringdown

Ringdown waveforms originate from a small perturbation of a spinning black hole (BH) and can be modelled as an exponential-damped sinusoid. The central frequency f of the fundamental quadrupolar mode and the quality factor Q depend on the mass M and the spin ($S = \hat{a}GM^2/c$) of the BH. They can be approximated by an analytic fit [1, 2] and are given by

$$f \approx 32 \text{ kHz} \left[1 - 0.63 (1 - \hat{a})^{\frac{3}{10}} \right] \left(\frac{M}{M_{\odot}} \right)^{-1} \quad \text{and} \quad Q \simeq 2 (1 - \hat{a})^{-\frac{9}{20}}. \quad (1)$$

The value of the dimensionless spin parameter \hat{a} is zero in the Schwarzschild limit (non-rotating BH) and 1 in the extreme Kerr limit (maximum rotational speed), so $Q > 2$.

The relative strain caused by any metric perturbation on the detector depends on the position of the BH in the sky and the relative orientation of its spin axis to the local zenith of

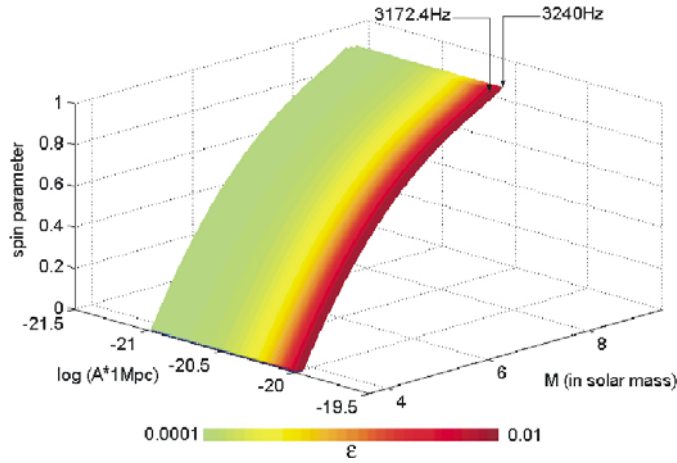


Figure 1. Volume formed by sets of parameters that correspond to frequencies varying from $f = 3172.5$ Hz to 3240 Hz.

the detector. The averaged strain produced by the tensorial GW components can be obtained by rms averaging over all possible angles and the result is $\langle h_{\text{GW}} \rangle_{\text{angle}} = Aq(t)$, where $q(t)$ is the damping function that depends on the rotation speed and on the central frequency of the BH,

$$q(t) = (2\pi)^{\frac{1}{2}} e^{-\pi ft/Q} \cos(2\pi ft), \quad (2)$$

for $t \geq 0$ (we set the time origin on $t = 0$). The amplitude A also depends on the fraction ϵ of the total mass–energy radiated and on the BH distance from the Earth (r), and it is given by

$$A \simeq 2.415 \times 10^{-21} Q^{-\frac{1}{2}} [1 - 0.63(1 - \hat{a})^{\frac{3}{10}}]^{-\frac{1}{2}} \left(\frac{\text{Mpc}}{r}\right) \left(\frac{M}{M_{\odot}}\right) \left(\frac{\epsilon}{0.01}\right)^{\frac{1}{2}}. \quad (3)$$

The quality factor roughly gives the number of coherent cycles for the waveform [3]. It affects the damping ($1/Q$), which decreases with increasing rotational speed. To generate the signal that was introduced in the model of the detector we chose one (among many) of the sets of parameters that made the central frequency of the BH quadrupolar normal mode coincident with one of the SCHENBERG resonant quadrupolar frequencies (3172.5 Hz, 3206.3 Hz and 3240 Hz). We obtain a certain volume in the space of parameters shown in figure 1 by fixing two boundary frequencies for the BH quadrupolar mode and then making those parameters vary. Consequently, any set of parameters inside that volume is within the SCHENBERG bandwidth.

2. The simulated signal

We chose $\epsilon = 0.01$, $M = 4M_{\odot}$ and $\hat{a} = 0.16$ to generate the signal that we used to calculate the signal-to-noise ratio. We believe that this efficiency is not overestimated since similar values have been found in the literature [3, 4]. Figure 2(a) shows the waveform $h(t)$ in the time domain. The Fourier transform of the impulse $h(t)$ is defined as

$$H(\omega) = \int_{-\infty}^{\infty} h(t) e^{-i\omega t} dt. \quad (4)$$

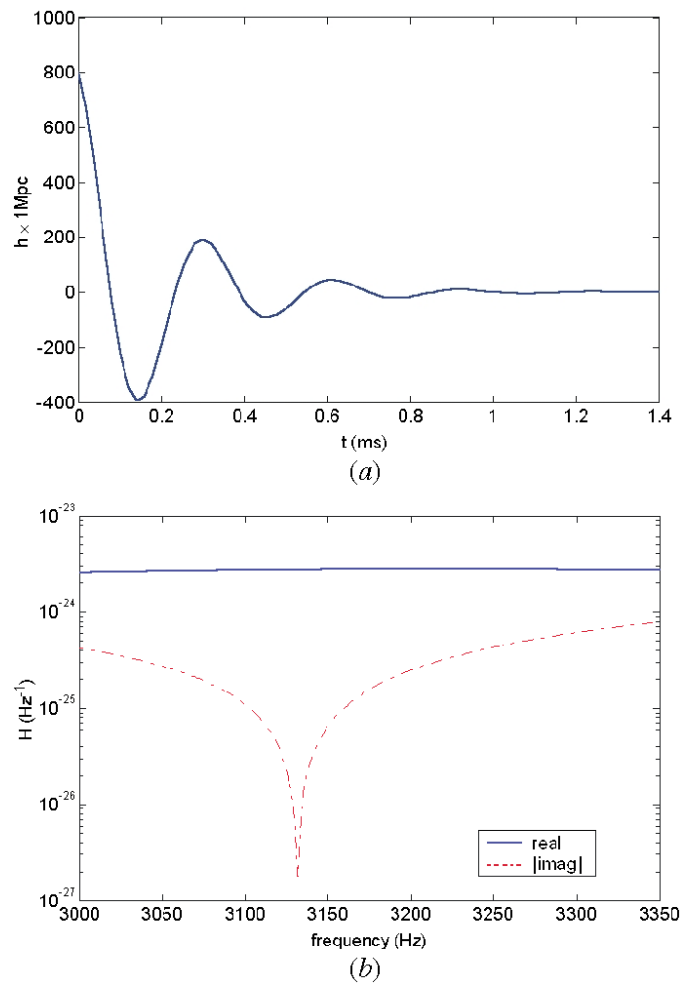


Figure 2. Waveform of a black hole ringdown (a) in the time domain and (b) in the frequency domain.

It represents the signal in the frequency domain and is shown in figure 2(b). This figure shows that the signal spectrum on the SCHENBERG bandwidth (3.17–3.24 kHz) is almost ‘white’. This is a direct consequence of the low value for the BH’s quality factor ($Q \approx 2.16$, for that simulated signal). For higher values of the quality factor the damping function tends to a sinusoid and a peak may appear in the spectrum. This would facilitate the detection of the signal.

3. The SCHENBERG model

We modelled the SCHENBERG detector by assuming a linear elastic theory. Adopting this approach we determined the mechanical response of the system and obtained an expression for the case when six 2-mode mechanical resonators are coupled to the antenna’s surface according to the arrangement suggested by Johnson and Merkowitz, the truncated icosahedron

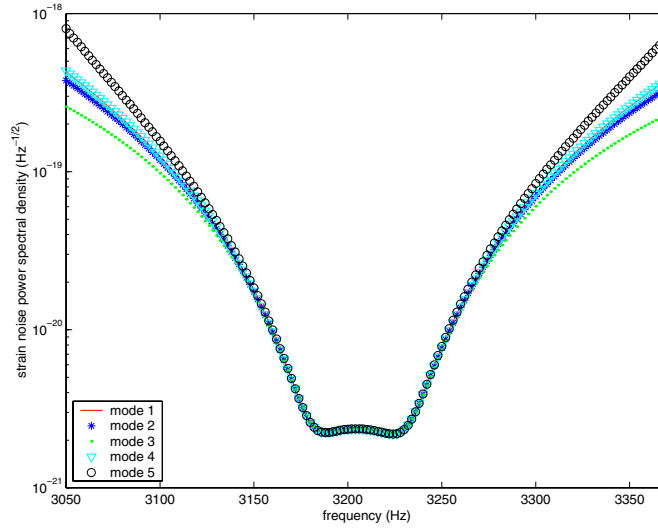


Figure 3. Sensitivity curve of SCHENBERG at 4.2 K for the quadrupolar normal modes m .

configuration [5, 6]. We found an analytic expression to calculate the spectral density for the mode channels, given by [7]

$$S_m^g(\omega) = |\xi_m(\omega)|^2 S_m^{\tilde{F}^S} + \sum_{j=1}^6 |\Omega_{mj}^{R_1}(\omega)|^2 S_j^{\tilde{F}^{R_1}} + \sum_{j=1}^6 |\Omega_{mj}^{R_2}(\omega)|^2 S_j^{\tilde{F}^{R_2}}. \quad (5)$$

The scalar $\xi_m(\omega)$ represents the transfer function of the sphere's internal forces \tilde{F}_m^S at angular frequency ω on mode m . The matrix elements $\Omega_{mj}^{R_i}(\omega)$ correspond to the response functions of channel m to the noise forces $\tilde{F}_j^{N_{R_i}}$ that are acting on the mode i of resonator j . S^X denotes the spectral density of the quantity X . In order to find equation (5), we assumed that all noise sources and possible signals were statistically independent so the cross terms could be neglected.

The GW effective force [7–9] that acts on the sphere (in the frequency domain) has spectral density

$$S_m^{\tilde{F}^{\text{GW}}}(\omega) = \left(\frac{1}{2}\omega^2 m_S \chi R\right)^2 S_m^{\tilde{h}}(\omega). \quad (6)$$

The sensitivity curve for mode m is given through

$$\tilde{h}_m(\omega) = \sqrt{\frac{1}{\left(\frac{1}{2}\omega^2 m_S \chi R\right)^2} \frac{S_m^g(\omega)}{|\xi_m(\omega)|^2}}. \quad (7)$$

Figure 3 shows the sensitivity curves for the five quadrupolar normal modes of the sphere. We obtained this curve assuming that no signal was present and that only the usual noises in this kind of detector (Brownian noise, serial noise, back-action noise and electronic phase and amplitude noises)³ were disturbing the antenna at 4.2 K. The absence of a signal made filtering unnecessary in this calculation. Also, we assumed a perfectly symmetric sphere, which implies identical transfer functions $\xi_m(\omega)$. Asymmetries on the sphere could make the transfer function of a mode different from the transfer function of the others.

³ For details on the parameters used in the Schenberg model see Aguiar *et al* and Frajuca *et al* in these proceedings.

4. Signal-to-noise ratio

Using the results in sections 2 (which inform about the signal) and 3 (which inform about the noise) it is easy to calculate the integrated signal-to-noise ratio (SNR) [10, 11]. For simplicity, we decided to use

$$\text{SNR} = \frac{1}{2\pi} \int_{-\infty}^{+\infty} \frac{|H(\omega)|^2}{S_N(\omega)} d\omega, \quad (8)$$

for SNR calculation. The quantity $S_N(\omega)$ represents the noise spectrum at angular frequency ω . Here we used the mean of the five sensitivity curves shown in figure 3. The integral in equation (8), which is dominated by the interval of SCHENBERG bandwidth, gives $\text{SNR} \gtrsim 1$ for the simulated signal when the BH's distance is $r \sim 20$ kpc.

5. Conclusion

If a low-spinning BH ($\hat{a} \sim 0.16$) with mass $\sim 4M_\odot$ and emission of about 1% of its mass-energy in the form of GW exists up to a distance of ~ 20 kpc, then the SCHENBERG detector is expected to observe it when operating at 4.2 K. In the calculation we did not take into account other possible dependences on the BH parameters except the known frequency-mass dependence. Strong dependences between ϵ and \hat{a} may make signals from high-spinning BHs much stronger which will give a better detectability rate.

Almost all theories claim the existence of BHs but experimental evidence is indirect (e.g. x-ray bursters in galactic bulge and disc). Certainly, it is not yet possible to predict the correct number of galactic BHs. However, some estimation can be performed, especially for binary systems which could merge and form such BHs (the coalescence rate for such systems is $\sim 10^{-5}$ – 10^{-4} year $^{-1}$ [13, 14], and it can be 10–30 times greater [15]). The initial mass function leads us to find that $\sim 1/8$ of the stars may have mass $\gtrsim 25M_\odot$, which could collapse into BHs [12] (supernova type II rate is ~ 1 – 3 century $^{-1}$). Moreover, these objects could be in binary systems (about a half) and they could be excited either by mass transfer from a companion or gravitational collisions with other objects (e.g. tidal friction on globular clusters [16]). The radius of ~ 20 kpc includes the galactic centre and the majority of the spiral arms and globular clusters, which are the most probable birthplaces for stellar BHs.

Gravitational wave detection presents one avenue for direct observation of black holes. So the detection of the kind of signal investigated in this work is an opportunity for gravitational wave astronomers to make essential discoveries about the black hole population in our galaxy.

Acknowledgments

This work was supported by FAPESP (under grant nos 1998/13468-9, 2001/14527-3 and 2003/02912-5), CNPq (under grant no 300619/92-8) and MCT/INPE. The authors also would like to thank the referees for useful suggestions.

References

- [1] Echeverria F 1989 *Phys. Rev. D* **40** 3194
- [2] Leaver E W 1985 *Proc. R. Soc. A* **402** 285
- [3] Creighton J D E 1999 *Phys. Rev. D* **60** 022001-1
- [4] Creighton J D E 1999 *GRASP 1.9.8—Users Manual* ed B Allen p 251 <http://www.lsc-group.phys.uwm.edu/~ballen/grasp-distribution>
- [5] Johnson W W and Merkowitz S M 1993 *Phys. Rev. Lett.* **70** 2367

-
- [6] Merkowitz S M and Johnson W W 1997 *Phys. Rev. D* **56** 7513
 - [7] Costa C A, Aguiar O D and Magalhães N S, in preparation
 - [8] Zhou C Z 1995 *Phys. Rev. D* **51** 2517
 - [9] Harry G M, Stevenson T R and Paik H J 1996 *Phys. Rev. D* **54** 2409
 - [10] Michelson P F and Taber R C 1981 *J. Appl. Phys.* **52** 4313
 - [11] Stevenson T R 1997 *Phys. Rev. D* **56** 564
 - [12] Podsiadlowski Ph, Rappaport S and Han Z 2003 *Mon. Not. R. Astron. Soc.* **341** 385
 - [13] Flanagan E E and Hughes S A 1998 *Phys. Rev. D* **57** 4535
 - [14] Flanagan E E and Hughes S A 1998 *Phys. Rev. D* **57** 4566
 - [15] Burgay M *et al* 2003 *Nature* **426** 531
 - [16] Blandford R D and Thorne K S 1979 Black hole astrophysics *General Relativity: an Einstein Centenary Survey* ed S Hawking (Cambridge: Cambridge University Press) p 454